Electronic Supplementary Material (ESI) for Inorganic Chemistry Frontiers.
This journal is © the Partner Organisations 2023

Supporting Information

A two-dimensional luminescent HOF containing the interpenetrating network structure with dual function: highly sensitive detection of methotrexate and multi-level information encryption

Chunyu Yang,† Xin Xu, † and Bing Yan*,†

†School of Chemical Science and Engineering, Tongji University, 1239 Siping Road, Shanghai 200092, China

* Corresponding author: Bing Yan, Email: byan@tongji.edu.cn

Experimental Section

Materials and Instruments: Unless otherwise stated, all reagents used in this work were reagent grades and purchased from commercial sources without further purification. Deionized water was used throughout the whole experiments. Tris[4-(1H-imidazol-1-yl)-phenyl]amine, methotrexate, methanol, adenosine 5'-monophosphate, urea, glucose, sodium bicarbonate, sodium chloride, potassium chloride, calcium chloride, magnesium chloride, histidine, serine, leucine, lysine, proline, cysteine, phenylalanine, ethylene glycol, polyvinyl alcohol and goat serum were procured from Sigma-Aldrich.

The powder X-ray diffraction (PXRD) patterns were recorded on Bruker D8 ADVANCE diffractometer employing Cu Kα radiation (40 mA and 40 kV). Fourier transform infrared (FT-IR) spectra were obtained by a Nexus 912 AO446 infrared spectrum radiometer in the wavenumber range of 4000 − 400 cm^{-1}. Thermogravimetric (TG) curves were measured on a TA TGA 55 system operating at a heating rate of 10 ^{o}C/min in the range of 25 ^{o}C up to 800 ^{o}C under N^2 atmosphere. The Automated Surface Area and Porosity Analyzer (BET) figure was obtained by Micromeritics ASAP 2460. The Commission International de l'Eclairage (CIE) coordinate were calculated by CIE1931 Chromaticity Coordinate Calculation according to the fluorescence emission spectra. The UV-vis absorption spectra were carried on an Agilent 8453 spectrometer. The photos of application in information encryption and decryption were collected by Ultraviolet Analyzer ZF-I and the power of the UV lamp was 6 W. The pH values of aqueous solutions were determined by an INESA PHS-25 pH meter with an E-201F pH composite electrode, which was carefully calibrated by standard buffer solution before testing. The water solution with various pH values was prepared by adding different content of HCl and NaOH in deionized water. The HOMO-LUMO energy levels were optimized by the B3LYP hybrid density functional and the basis set was 6-31G(d).

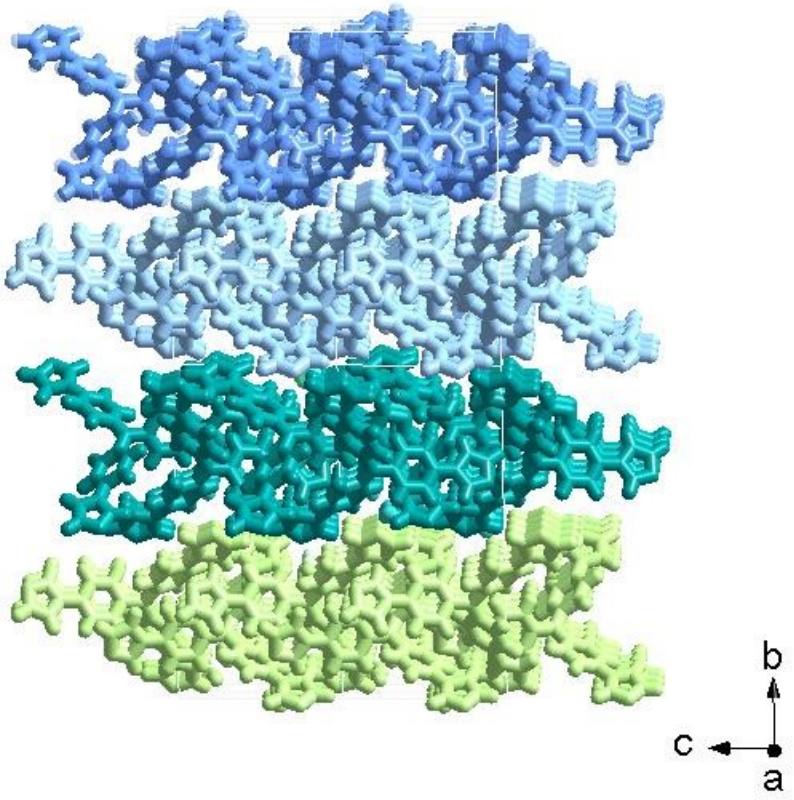

Fig. S1 The 3-dimensional framework of HOF-TIA along the *a* axis. The molecular stacking modes of adjacent layers are opposite.

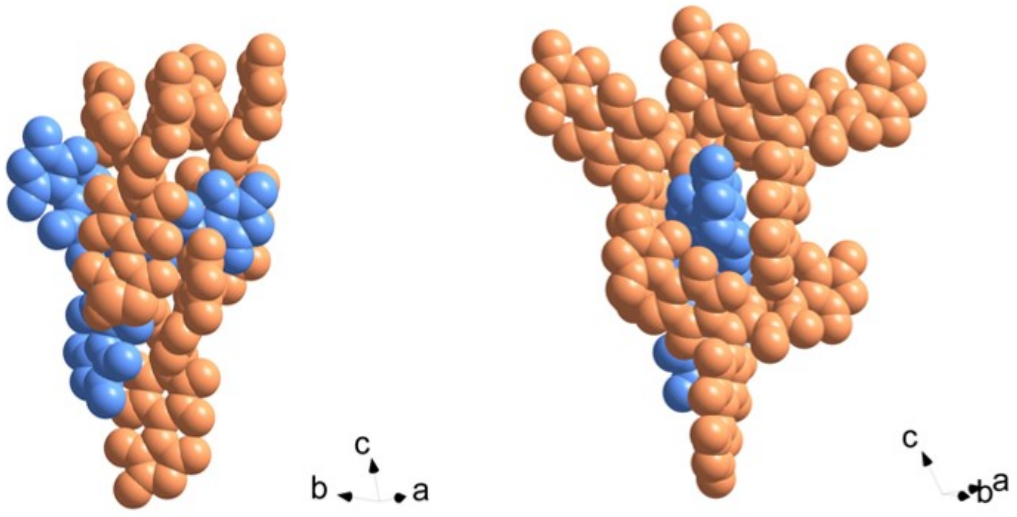

Fig. S2 Schematic diagram of TIA molecular crossover of different arrangements in HOF-TIA framework.

Table S1 The crystallographic data of **HOF-TIA.**

Crystal data	**HOF-TIA**
CCDC number	2221028
Crystal system	monoclinic
Space group	$P2_1/c$
Molecular formula	C27H21N7O3
Formula weight	497.55
a / Å	9.998(5)
b / Å	22.169(11)
c / Å	11.873(7)
α/°	90
β/°	113.267(2)
γ/°	90
Volume/ Å^3	2417.7(2)
Z	4
Density/ g/cm^3	1.36685
GOF on **F2**	1.019
R1a[I>2σ(I)]	0.0515
ωR2b[I>2σ(I)]	0.1343

Table S2 The bond angle and distance between two atoms for hydrogen bonds in HOF-TIA.

hydrogen bonds	bond angle	atoms	distance
O3-H3···O1	173.64	O3-O1	2.8174
O1-H1···N1	172.25	O1-N1	2.8045
O2-H3···C3	154.94	O2-C3	3.3715

The angle between plane 1 (purple) and plane 2 (green) is 5.154 °, the angle between plane 1 (purple) and plane 3 (yellow) is 64.635 °, the angle between plane 2 (green) and plane 3 (yellow) is 69.865 °. Plane 1: N1, C1, C2, N2 and C3 atoms; Plane 2: N3, C26, C17, N4 and C18 atoms; Plane 3: N5, C25, C26, N6 and C27 atoms.

Table S3 Summary of the methods for sensing MTX.

Method	Linear range (μM)	DL (μM)	Ref.
Electrochemical	0.70–100	0.070	[R_{S1}]
Electrochemical	2.2–25	0.090	[R_{S2}]
Fluorescence	0–0.5	0.0605	[R_{S3}]
Fluorescence	0.1–2	0.030	[R_{S4}]
Fluorescence	0.05–1	0.042	[R_{S5}]
SERS	0–80	2.36	[R_{S6}]
SERS	0.2–2	0.17	[R_{S7}]

[R_{S1}] E. Asadian, S. Shahrokhian, A. Iraji Zad, F.G. Bidkorbeh, Glassy Carbon Electrode Modified with 3D Graphene–Carbon Nanotube Network for Sensitive Electrochemical Determination of Methotrexate, *Sens. Actuators B Chem.,* 2017, **239**, 617–627.

[R_{S2}] Y. Göksel, K. Zor, T. Rindzevicius, B.E. Thorhauge Als-Nielsen, K. Schmiegelow, A. Boisen, Quantification of Methotrexate in Human Serum Using SurfaceEnhanced Raman Scattering—Toward Therapeutic Drug Monitoring, *ACS Sens.,* 2021, **6**, 2664–2673.

[R_{S3}] M.H. Bruhn, L.D.F. Nielsen, K.V. Gothelf, Rapid Detection of Drugs in Human Plasma Using a Small-Molecule-Linked Hybridization Chain Reaction, *ACS Sens.,* 2018, **3**, 1706–1711.

[R_{S4}] J. He, J. Wang, M. Zhang, G. Shi, Selection of a Structure-Switching Aptamer for the Specific Methotrexate Detection, *ACS Sens.,* 2021, **6**, 2436–2441.

[R_{S5}] L. Yang, J. Ge, D. Ma, J.L. Tang, H.Q. Wang, Z.H. Li, MoS_2 Quantum Dots as Fluorescent Probe for Methotrexate Detection, *Spectrochim. Acta. A Mol. Biomol. Spectrosc.,* 2022, **279**, 121443.

[***R***$_{S6}$] A. Subaihi, D.K. Trivedi, K.A. Hollywood, J. Bluett, Y. Xu, H. Muhamadali, D.I. Ellis, and R. Goodacre, Quantitative Online Liquid Chromatography–Surface-Enhanced Raman Scattering (LC-SERS) of Methotrexate and its Major Metabolites, Anal. Chem*.,* **2017,** ***89***, 6702–6709.

[R_{S7}] I.J. Hidi, A. Mühlig, M. Jahn, F. Liebold, D. Cialla, K. Weber, J. Popp, LOC-SERS: towards Point-of-care Diagnostic of Methotrexate, *Anal. Methods,* 2014, **6**, 3943–3947.

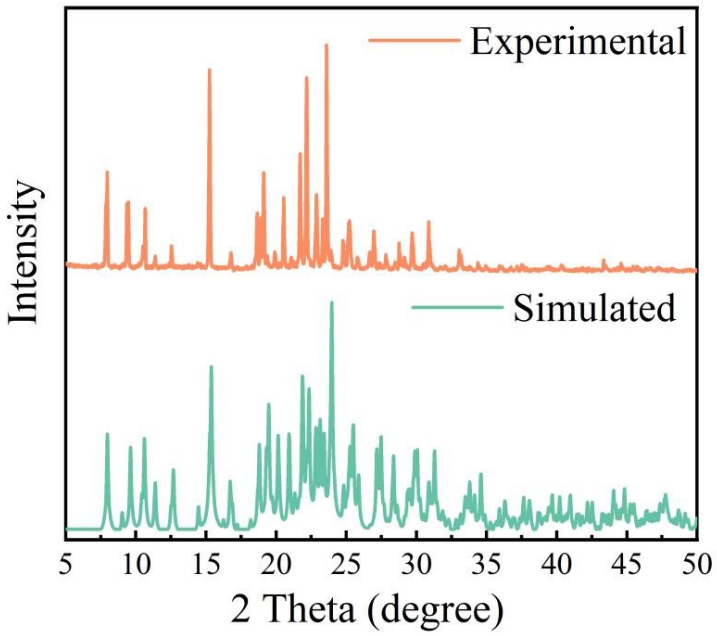

Fig. S3 Experimental PXRD patterns of HOF-TIA (orange line) and simulated PXRD pattern (green line).

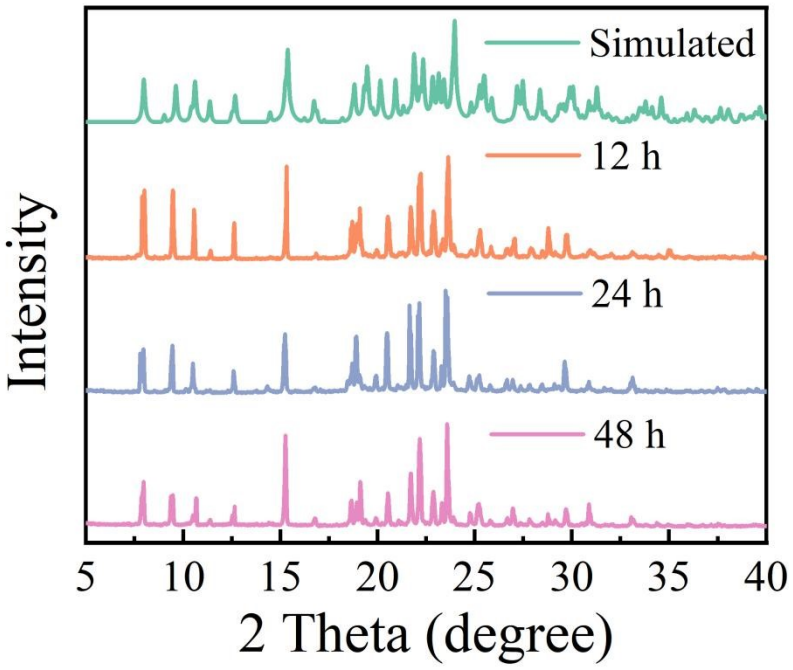

Fig. S4 PXRD patterns of HOF-TIA powder soaked in water

(for 12 h, 24 h and 48 h).

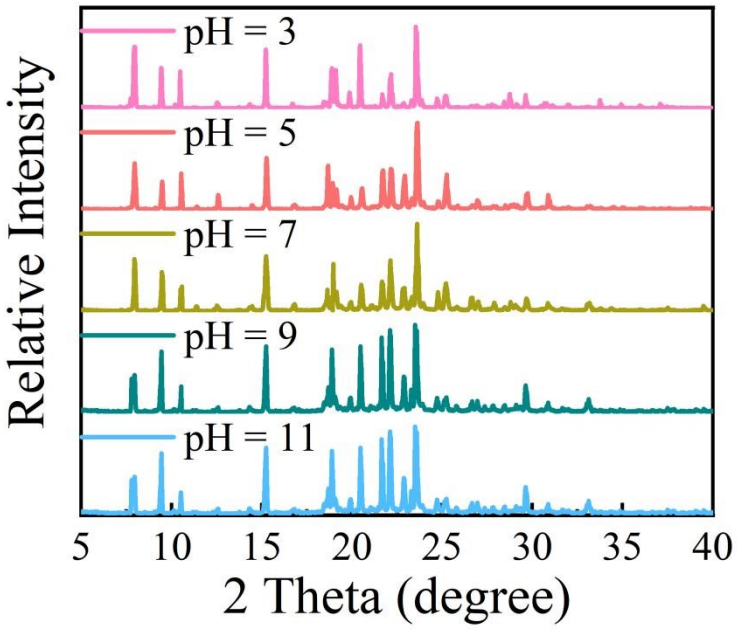

Fig. S5 PXRD patterns of HOF-TIA powder soaking in different pH solution. (pH = 3, 5, 7, 9, 11) The water solution with various pH values was prepared by adding different content of HCl and NaOH in deionized water.

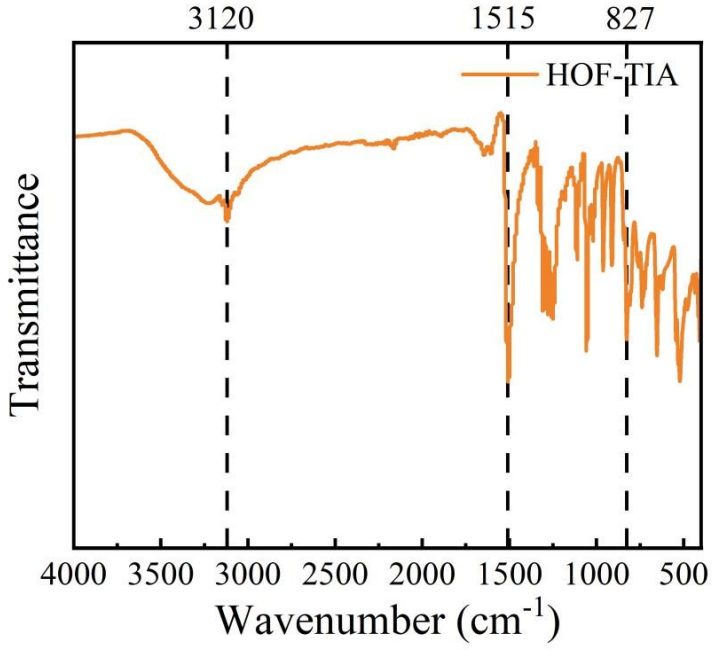

Fig. S6 Infra-red (IR) spectrum of HOF-TIA powder.

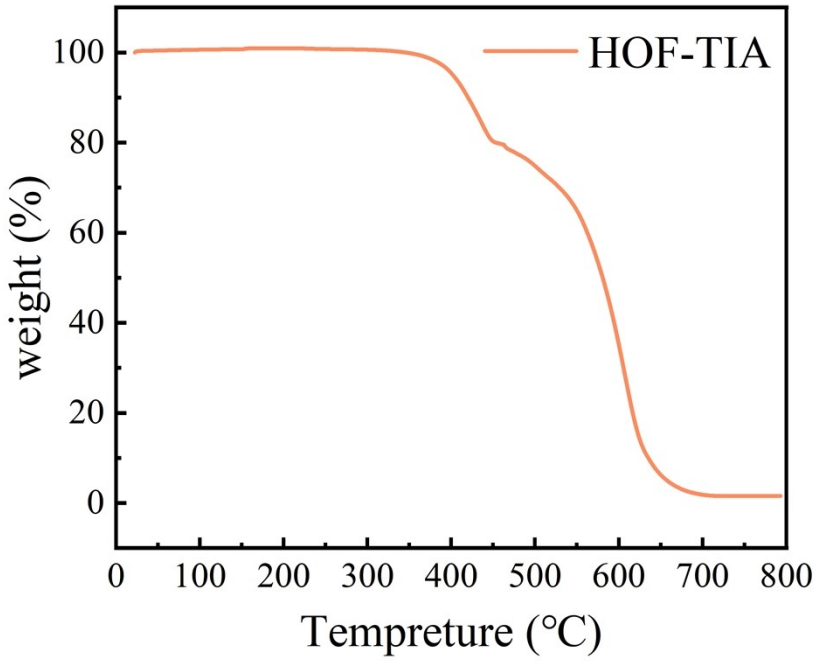

Fig. S7 The TG profiles of HOF-TIA.

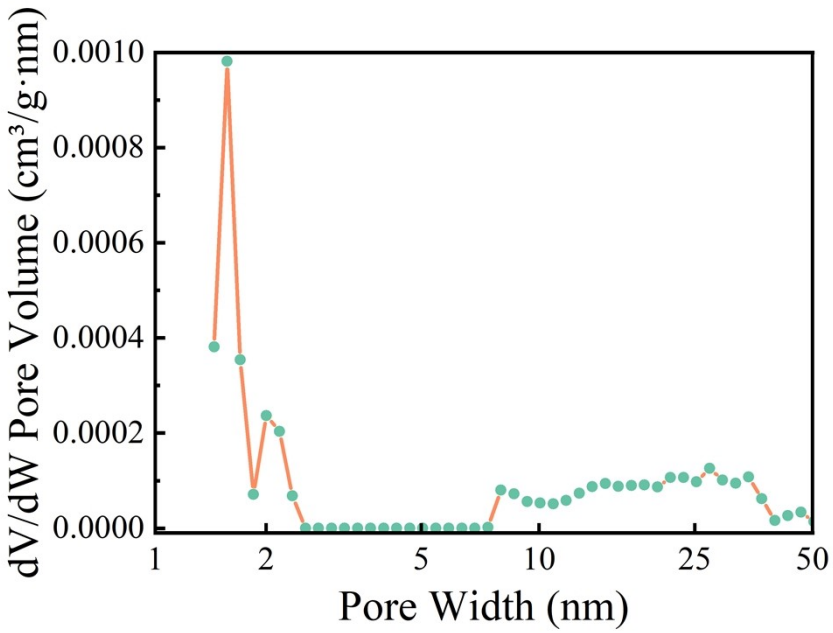

Fig. S8 Pore size distribution curve of HOF-TIA. The value of the pore volume is 0.00510 cm3 and the value of the total volume is 0.09189 cm3. The calculated porosity is 5.55%.

Porosity (P_t) = Pore volume (V_p) / Total volume (V_t) (Formula S1)

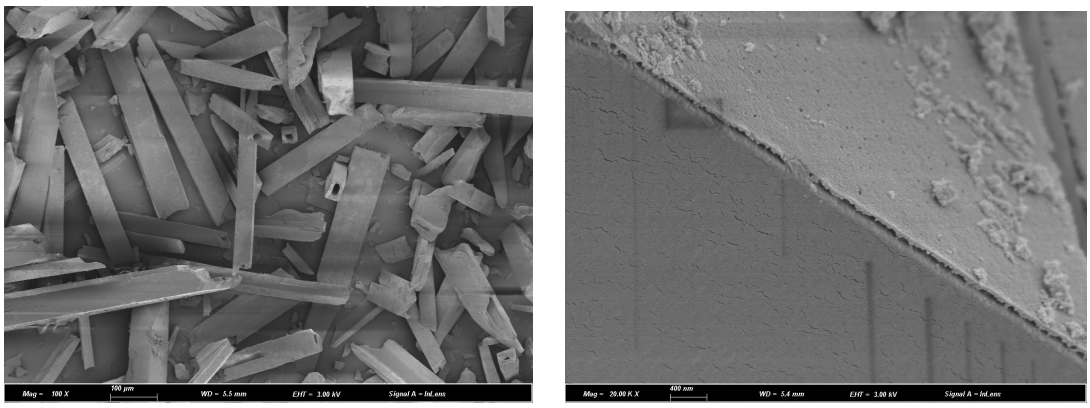

Fig. S9 SEM images of HOF-TIA. (The picture on the right shows the surface of the crystal with the presence of some black dots, probably a reflection of HOF-TIA as a microporous material.)

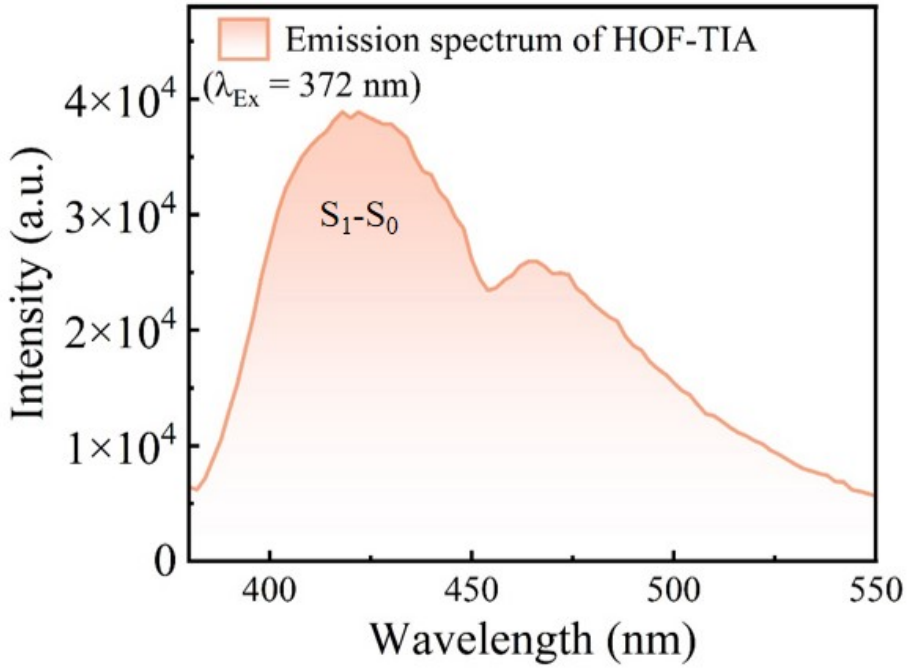

Fig. S10 Emission spectrum of HOF-TIA powder. (λ_{ex} = 372 nm)

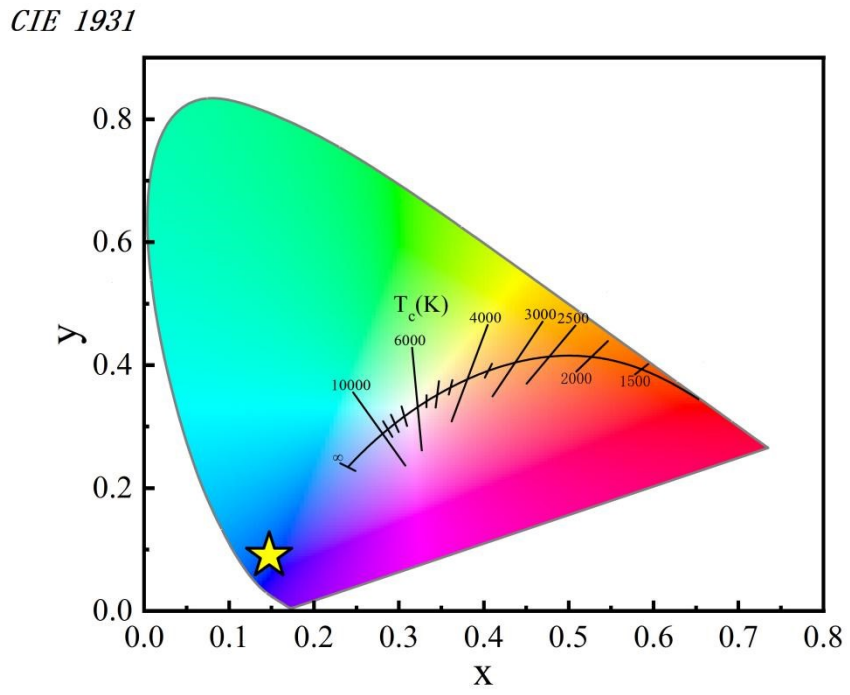

Fig. S11 CIE diagram of HOF-TIA powder at 372 nm excitation.

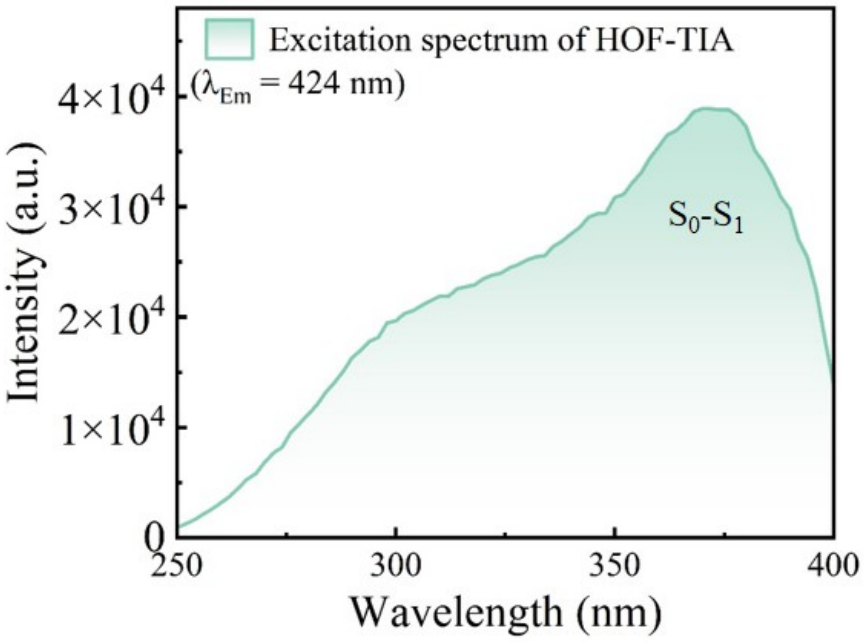

Fig. S12 Excitation spectrum of HOF-TIA powder. (λ_{em} = 424 nm)

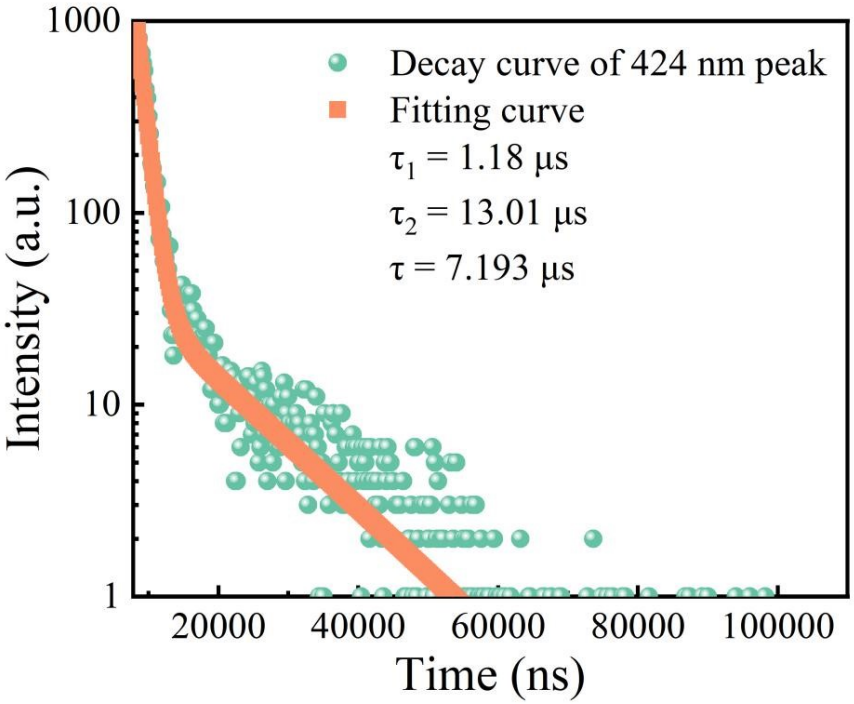

Fig. S13 Emission decay profile of the 424 nm peak for HOF-TIA powder.

(λ_{ex} = 372 nm).

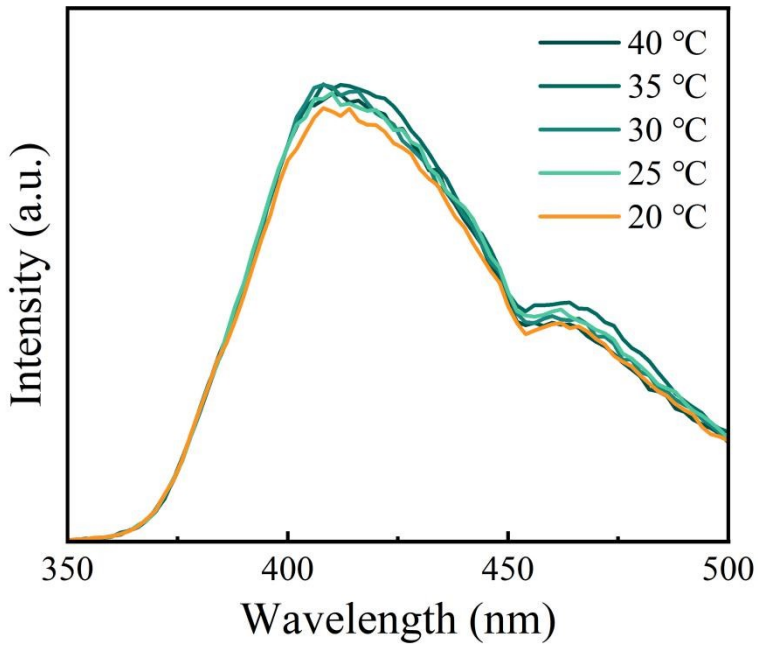

Fig. S14 Emission spectrum of HOF-TIA in deionized water at different tempreture (T = 20, 25, 30, 35 and 40 ℃).

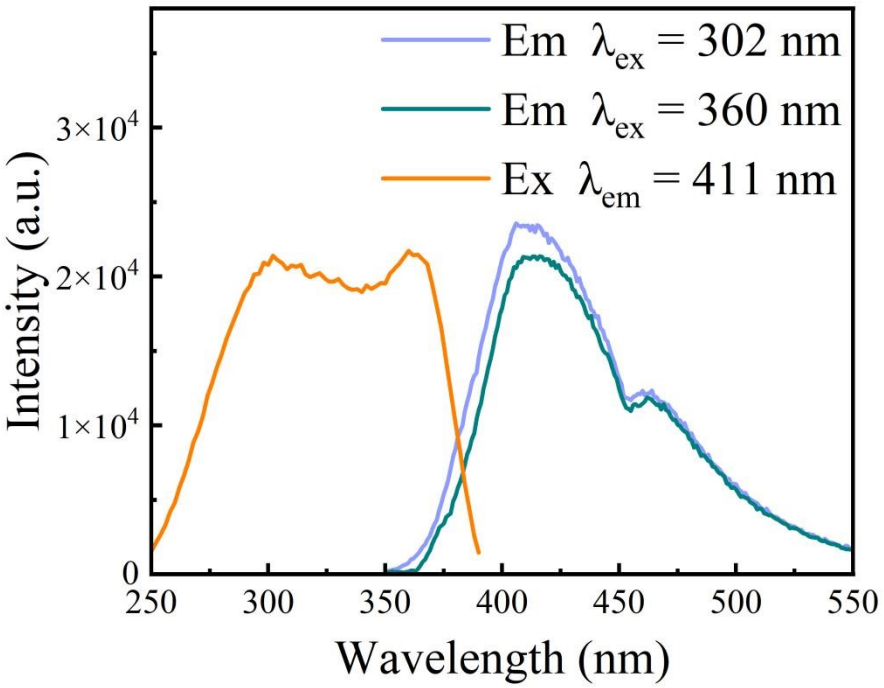

Fig. S15 Excitation and emission spectra of aqueous suspensions of HOF-TIA.

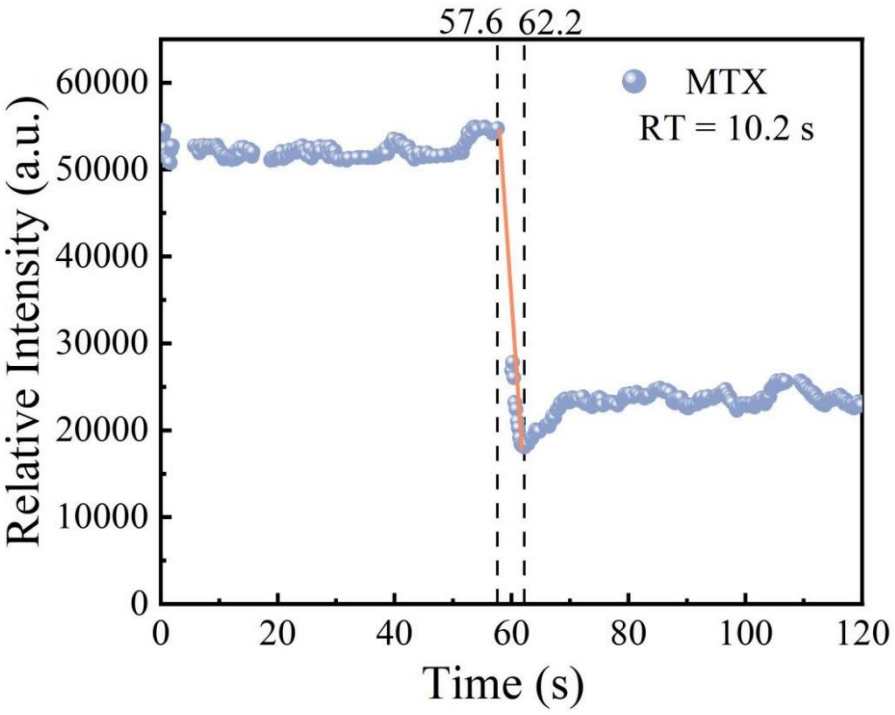

Fig. S16 Response time of HOF-TIA to MTX. (RT = 10.2 s)

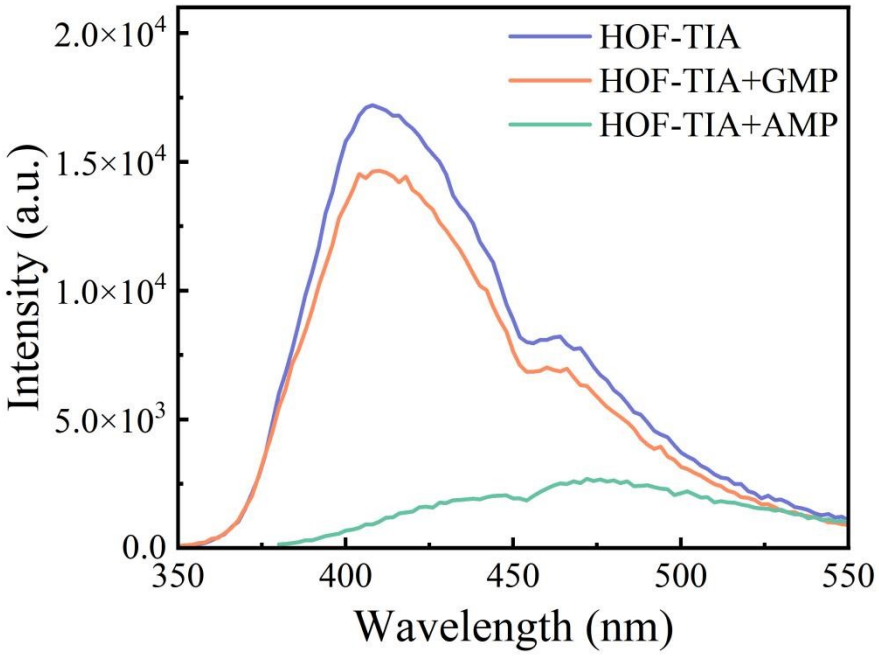

Fig. S17 Emission spectrum of HOF-TIA added to AMP and GMP solutions respectively.

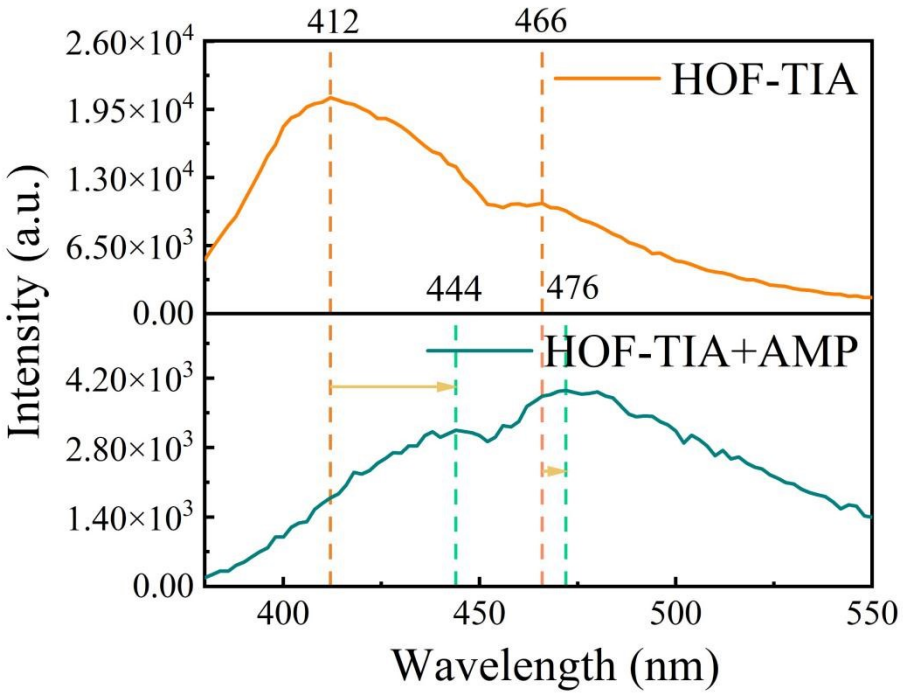

Fig. S18 The distinction between the emission spectrum of HOF-TIA and HOF-TIA with AMP solution.

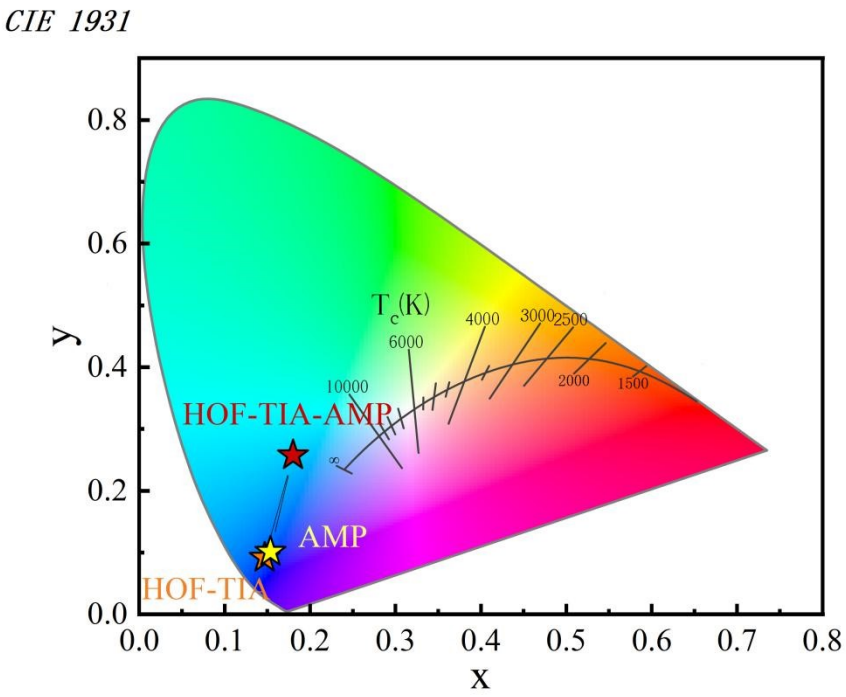

Fig. S19 CIE 1931 diagram illustrating coordinates shift of HOF-TIA after interacting with AMP from (0.147, 0.092) to (0.180, 0.257) and the ordinary coordinates of AMP (0.153,0.101).

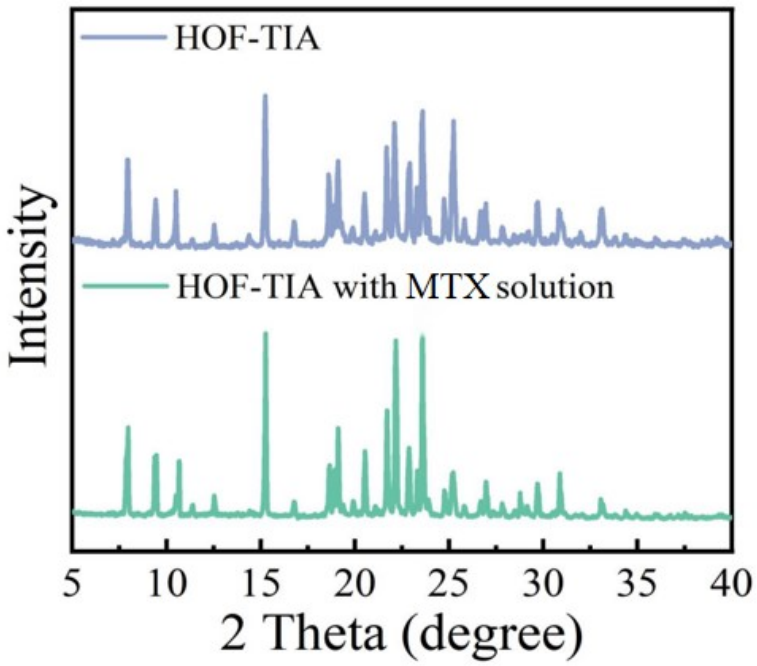

Fig. S20 PXRD patterns of HOF-TIA (blue line) and HOF-TIA with MTX solution (green line).

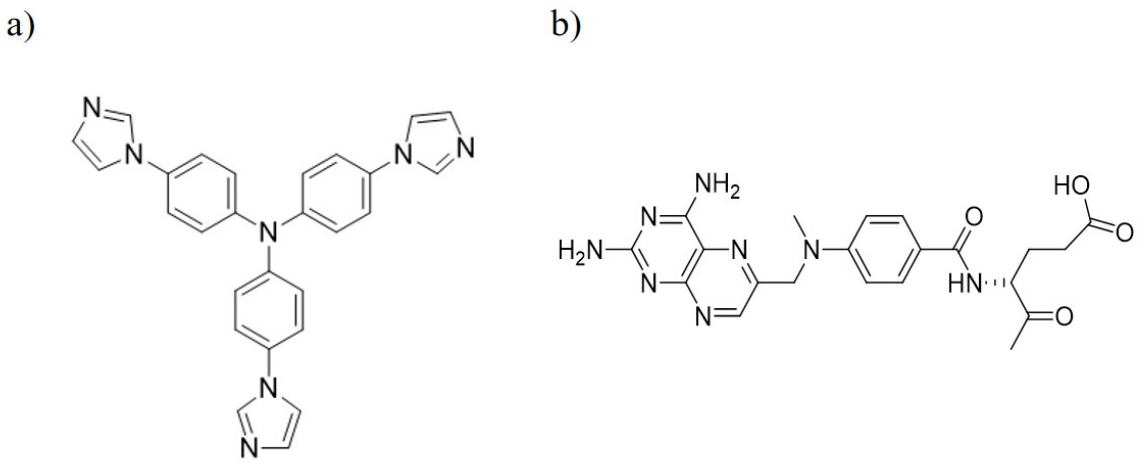

Fig. S21 The structural formula of TIA and MTX.

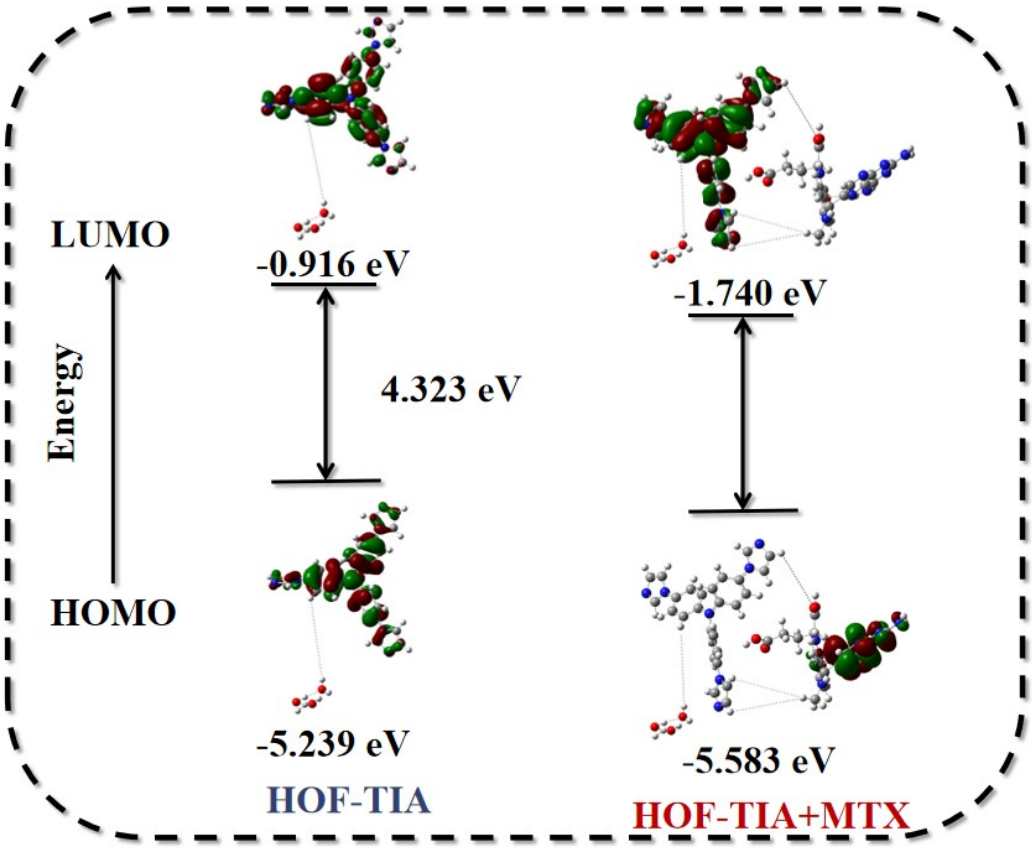

Fig. S22 LUMO and HOMO of HOF-TIA molecule fragment and MTX.

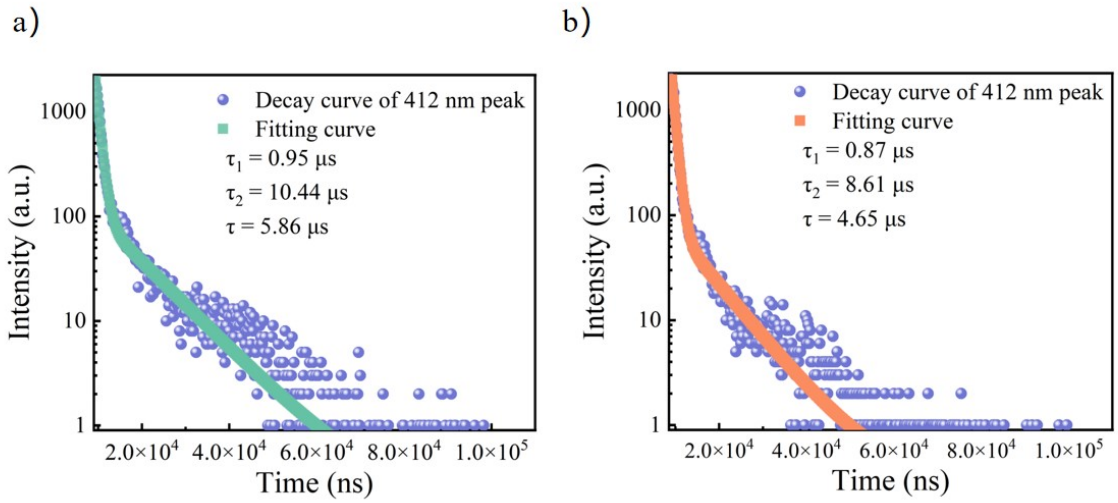

Fig. S23 Emission decay profiles of the 411 nm peak for HOF-TIA. (b) Emission decay profiles of the 411 nm peak for HOF-TIA with AMP solution. (λ_{ex} = 360 nm)

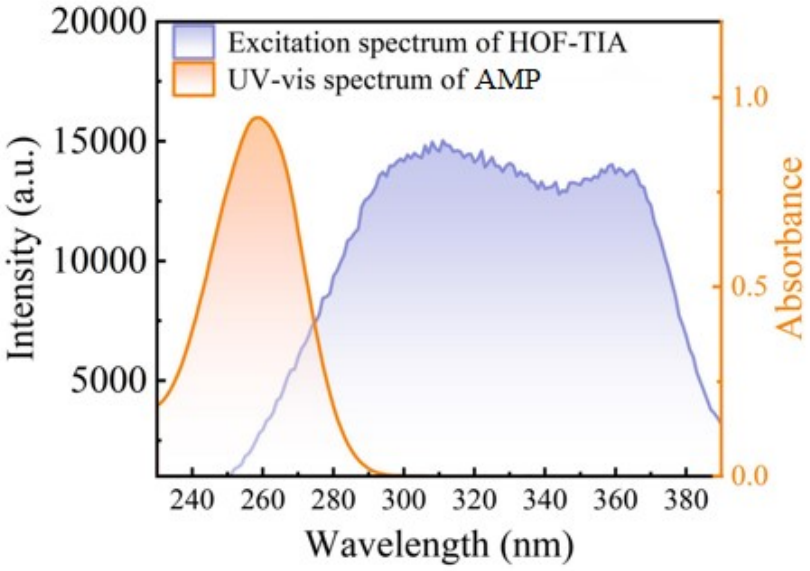

Fig. S24 The UV absorption spectra of AMP solution and the excitation spectrum of HOF-TIA.

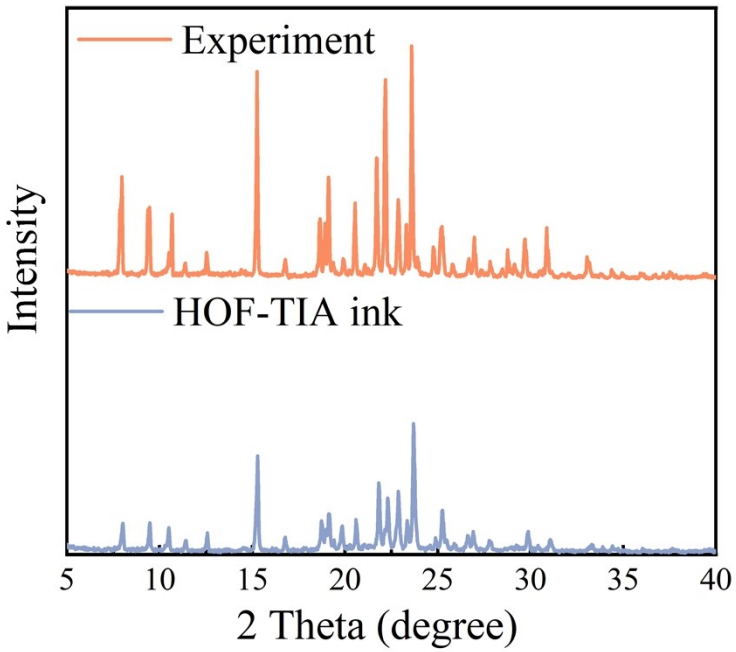

Fig. S25 PXRD patterns of HOF-TIA before and after the production of ink